

One Framework to Register Them All: PointNet Encoding for Point Cloud Alignment

Vinit Sarode^{1*}, Xueqian Li^{1*}, Hunter Goforth³, Yasuhiro Aoki², Animesh Dhagat,¹

Rangaprasad Arun Srivatsan⁴, Simon Lucey^{1,3}, Howie Choset¹

¹Carnegie Mellon University and ²Fujitsu Laboratories Ltd. and ³Argo AI. and ⁴Apple.
 {vsarode, xueqianl, adhagat}@andrew.cmu.edu, aoki-yasuhiro@fujitsu.com
 {hgoforth, slucey, choset}@cs.cmu.edu, aruns@apple.com

Abstract

PointNet has recently emerged as a popular representation for unstructured point cloud data, allowing application of deep learning to tasks such as object detection, segmentation and shape completion. However, recent works in literature have shown the sensitivity of the PointNet representation to pose misalignment. This paper presents a novel framework that uses PointNet encoding to align point clouds and perform registration for applications such as 3D reconstruction, tracking and pose estimation. We develop a framework that compares PointNet features of template and source point clouds to find the transformation that aligns them accurately. In doing so, we avoid computationally expensive correspondence finding steps, that are central to popular registration methods such as ICP and its variants. Depending on the prior information about the shape of the object formed by the point clouds, our framework can produce approaches that are shape specific or general to unseen shapes. Our framework produces approaches that are robust to noise and initial misalignment in data and work robustly with sparse as well as partial point clouds. We perform extensive simulation and real-world experiments to validate the efficacy of our approach and compare the performance with state-of-art approaches. Code is available at <https://github.com/vinit5/pointnet-registration-framework>.

1 Introduction

3D point clouds are ubiquitous today, thanks to the development of low-cost and reliable lidar, stereo cameras and structured light sensors. As a result there has been a growing interest in developing algorithms for performing classification, segmentation, tracking, mapping, etc. directly using point clouds. However, the inherent lack of structure presents difficulties in using point clouds directly in deep learning architectures. Recent developments such as PointNet (Qi et al. 2017a) and its variants (Qi et al. 2017b) have been instrumental in overcoming some of these difficulties, resulting in state-of-the-art methods for object detection and segmentation tasks (Qi et al. 2018; Yuan et al. 2018a).

Prior works (Yuan et al. 2018a; Aoki et al. 2019) have observed that robust performance of PointNet requires minimal misalignment of the point clouds with respect to a

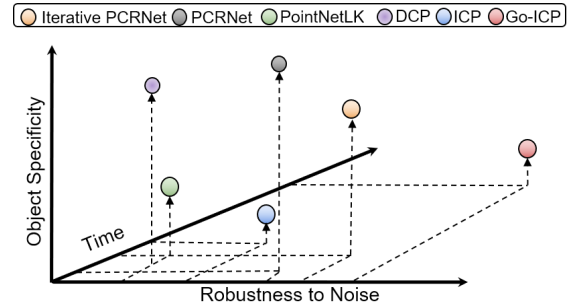


Figure 1: ‘No free lunch’ in point cloud registration. Comparison of different registration methods based on their robustness to noise and computation time with respect to object specificity. The iterative version of point cloud registration network (PCRNet) exploits object specificity to produce accurate results. The PCRNet without iterations is computationally faster and more robust to noise, but compromises a little on accuracy. Deep closest point (Wang and Solomon 2019) is also computationally fast, but not as robust to noise. While PointNetLK (Aoki et al. 2019) exhibits good generalizability to unseen objects. ICP (Besl and McKay 1992) is object-shape agnostic and slow for large point clouds, while Go-ICP (Yang et al. 2016) is computationally expensive.

canonical coordinate frame. While this is present in synthetic datasets such as *ModelNet40* (Wu et al. 2015), real world data is seldom aligned to some canonical coordinate frame. Inspired by recent works on iterative transformer network (IT-Net) (Yuan et al. 2018a) and PointNetLK (Aoki et al. 2019), this work introduces a framework for estimating the misalignment between two point clouds using PointNet as an encoding function. It is worth noting that our approach can directly process point clouds for the task of registration, without the need for hand crafted features (Rusu, Blodow, and Beetz 2009; Gelfand et al. 2005), voxelization (Maturana and Scherer 2015; Gojcic et al. 2019) or mesh generation (Wang et al. 2018). Our framework provides approaches that can utilize prior knowledge of the shape of the object being registered, to robustly deal with noise, sparse measurements and incomplete data. Our framework also provides additional context for PointNetLK (see Sec. 3.2 for more de-

*equal contribution

tails). It is worth emphasizing, that we do not propose a single registration technique that outperforms all state-of-the-art methods. Instead we propose a framework that generates a number of registration approaches, including some that already exist in literature. The performance of the various approaches produced by our framework depend on factors such as the prior information about the shape of the object, noise in the measurements and computation time (see Fig. 1).

Our approach uses PointNet in a siamese architecture to encode the shape information of a template and a source point cloud as feature vectors, and estimates the pose that aligns these two features using data driven techniques. The pose estimation from the features are carried out either using a number of fully connected (FC) layers or using classical alignment techniques such as Lucas-Kanade (LK) algorithm (Lucas and Kanade 1981; Baker and Matthews 2004). The LK algorithm results in good generalizability, but is not robust to noise. The FC layers are robust to noise, but not generalizable to shapes unseen during training.

Using shape-specific prior information in the training phase allows us to be robust to noise in the data, compared to shape agnostic methods such as iterative closest point (ICP) (Besl and McKay 1992) and its variants (Rusinkiewicz and Levoy 2001). Unlike ICP, our approach does not require costly closest point correspondence computations, resulting in improved computational efficiency and robustness to noise. Further, the approach is fully differentiable which allows for easy integration with other deep networks and can be run directly on GPU without need for any CPU computations.

Our contributions are (1) presenting a novel framework for point cloud alignment which utilize PointNet representation for effective correspondence-free registration, and (2) a thorough experimental validation of our approaches including comparison against popular and state-of-the-art registration methods (both conventional and learning-based approaches), on both simulated and real-world data.

2 Related Work

Classical registration. Iterative Closest Point (ICP) remains one of the most popular techniques for point cloud registration, as it is straightforward to implement and produces adequate results in many scenarios (Besl and McKay 1992). Extensions of ICP have increased computational efficiency (Rusinkiewicz and Levoy 2001; Srivatsan et al. 2019) and improved accuracy (Yang et al. 2016). However, nearly all ICP variants rely on explicit computation of closest point correspondences, a process which scales poorly with the number of points. Additionally, ICP is not differentiable (due to the requirement to find discrete point correspondences) and thus cannot be integrated into end-to-end deep learning pipelines, inhibiting the ability to apply learned descriptors for alignment.

Interest point methods compute and compare local descriptors to estimate alignment (Gelfand et al. 2005; Guo et al. 2014). These methods have the advantage of being computationally favorable, however, their use is often limited to point cloud data having identifiable and unique features which are persistent between point clouds that are

being registered (Makadia, Patterson, and Daniilidis 2006; Ovsjanikov et al. 2010; Rusu, Blodow, and Beetz 2009).

Globally optimal methods (Izatt, Dai, and Tedrake 2017; Maron et al. 2016) seek to find optimal solutions which cannot reliably be found with iterative techniques such as ICP. Unfortunately, these techniques are characterized by extended computation times, which largely precludes their use in applications requiring real-time speed. A representative example which we use as a baseline is Go-ICP (Yang et al. 2016), a technique using branch-and-bound optimization.

PointNet. PointNet is the first deep neural network which processes point clouds directly (Qi et al. 2017a), as opposed to alternative representations such as 2D image projections of objects (Xiang et al. 2018; Bristow, Valmadre, and Lucey 2015; Georgakis et al. 2018), voxel representations (Maturana and Scherer 2015; Wu et al. 2015; Zhou and Tuzel 2018) or graph representations (Wang et al. 2018). Within larger network architectures, PointNet has proven to be useful for tasks including classification, semantic segmentation, object detection (Qi et al. 2018), flow estimation (Liu, Qi, and Guibas 2019), and completion of partial point clouds (Yuan et al. 2018b). An extension to PointNet for estimating local feature descriptors is described in (Qi et al. 2017b). Yuan et al. introduced iterative transformer network (IT-Net) which uses PointNet to estimate a canonical orientation of point clouds to increase classification and segmentation accuracy. Global descriptors from PointNet are used in (Angelina Uy and Hee Lee 2018) for place recognition from 3D data.

Learned registration. Early learning-based approaches use a combination of hand-crafted and learned features and learned map sets for the task of point cloud registration (Vongkulbhisal et al. 2018). Deep auto-encoders are used to extract local descriptors for registration of large outdoor point clouds in (Elbaz, Avraham, and Fischer 2017). Yew and Lee introduced a network which learns both interest point detection and descriptor computation, for a descriptor-matching registration approach. More recently Lu et al. developed Deep-ICP, an approach that learns correspondences between point clouds and then uses an SVD to align the points similar to ICP (Lu et al. 2019). A major shortcoming of all these approaches is they do not typically scale well with increase in the number of points being registered, and lack generalization due to the feature vector and registration maps both being learned.

PointNetLK (Aoki et al. 2019), which performs registration of arbitrary point clouds by minimizing the distance between the fixed-length, global descriptors produced by PointNet, is the most closely related to our work and serves as a baseline. Another work that comes close to ours is the siamese network used by Zhou et al. to estimate the orientation between two point clouds (Zhou et al. 2019). As an alternate to PointNet encoding, Wang et al. perform convolution operations on the edges that connect neighboring point pairs, by using a local neighborhood graph (Wang et al. 2018). They introduced a network called Deep Closest

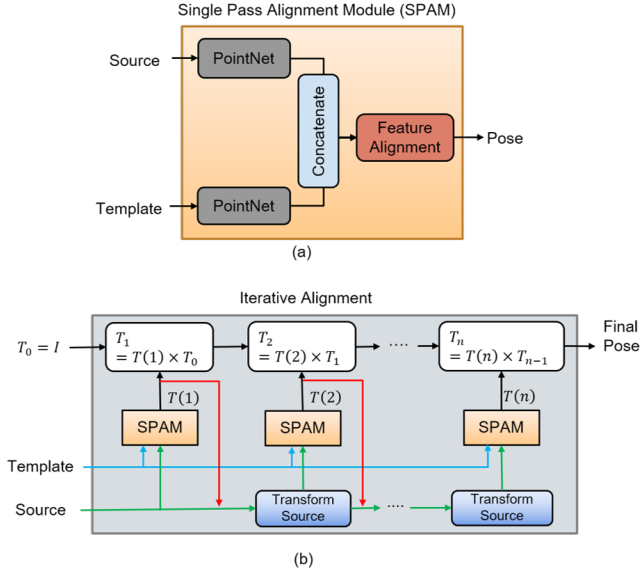


Figure 2: (a) Single Pass Alignment Module (SPAM): This module estimates the pose in a single pass, from a source and template point cloud. PointNet is used in a siamese architecture to extract a global feature vectors from both source and template. The point cloud alignment problem is posed in terms of alignment of the features. This circumvents the problem of finding explicit point correspondences. Different choices for the feature alignment algorithms gives rise to different approaches with their inherent advantages and disadvantages. (b) Iterative Alignment: The output of SPAM can be iteratively improved. After each iteration, the source point cloud is transformed using the pose estimated from the previous iteration. After performing n iterations, the poses from each iteration are combined to find the overall transformation.

Point (DCP), which uses this graph to perform point cloud alignment (Wang and Solomon 2019). We also present comparisons to this method in this work.

In addition to the above mentioned methods, there are several learning-based approaches that perform alignment with RGB-D data (Pais et al. 2019; Insafutdinov and Dosovitskiy 2018; Li et al. 2018; Wang et al. 2019). Since we use only point cloud data and no associated RGB information in this work, we restrict our comparisons to methods that use only point clouds for alignment.

3 Method

Point clouds are highly unstructured with ambiguities in the order permutations. While performing classification using PointNet, a symmetric pooling function such as max pool is used to afford invariance to input permutation (see (Qi et al. 2017a) for more details). The output vector of the symmetry function is referred to as a global feature vector. We denote the template point cloud \mathbf{P}_T and source \mathbf{P}_S , and the PointNet function ϕ . Since the global feature vectors contain the information about the geometry as well as the orientation of the point clouds, the transformation between two point

clouds can be obtained by comparing the feature vectors. In other words, we calculate the rigid-body transformation $\mathbf{T} \in SE(3)$, that minimizes the difference between $\phi(\mathbf{P}_S)$ and $\phi(\mathbf{P}_T)$.

3.1 Single Pass Alignment Module

This section introduces an alignment module that is central to the framework (see Fig. 2(a)). This module takes as input a point cloud data obtained from a sensor, which is referred to as the *source* and a point cloud corresponding to the known model of the object to be registered, which is referred to as the *template*. Both source \mathbf{P}_S and template \mathbf{P}_T are given as input to a PointNet module. The PointNet internally has several layers of multi-layered perceptrons (MLPs), which are arranged in a Siamese architecture (Held, Thrun, and Savarese 2016). A symmetric max-pooling function is used to find the global feature vectors $\phi(\mathbf{P}_S)$ and $\phi(\mathbf{P}_T)$. Weights are shared between the MLPs used for source and template. The model consists of five MLPs having size 64, 64, 64, 128, 1024. The global features are concatenated and given as an input to a feature alignment module. This module either uses classical alignment techniques or uses data driven techniques to learn the alignment between the features.

3.2 Iterative Alignment

Inspired by iterative schemes for alignment problem such as (Baker and Matthews 2004; Besl and McKay 1992; Li et al. 2018), etc., we use SPAM to refine the pose estimate after each iteration and obtain an accurate alignment between the source and template point clouds (see Fig. 2(b)).

In the first iteration, original source and template point clouds are given to SPAM which predicts an initial alignment $\mathbf{T}(1) \in SE(3)$ between them. For the next iteration, $\mathbf{T}(1)$ is applied to the source point cloud and then the transformed source and the original template point clouds are given as input to the SPAM. After performing n iterations, we find the overall transformation between the original source and template point clouds by combining all the poses in each iteration: $\mathbf{T} = \mathbf{T}(n) \times \mathbf{T}(n-1) \times \dots \times \mathbf{T}(1)$.

Depending on the choice of feature alignment algorithm, number of iterations, and choice of loss functions several different approaches can be produced by this framework. We explain three approaches in the next section, namely: PCRNet, i-PCRNet and PointNetLK.

PCRNet This section introduces the point cloud registration network (PCRNet) architecture. The PCRNet is a single pass pose estimator, which uses data driven techniques to align the PointNet features. Five fully connected layers of size 1024, 1024, 512, 512, 256 are used along with an output layer of the dimension of the parameterization chosen for the pose. We tried using lesser number of FC layers, but the performance of the network was poor.

The transformation \mathbf{T} which aligns $\phi(\mathbf{P}_S)$ and $\phi(\mathbf{P}_T)$ is estimated with a single forward pass, or single-shot, through the network. The single-shot design lends itself particularly well to high-speed applications, which will be discussed further in Sec. 4.

Iterative PCRNet In this section, we introduce iterative PCRNet (i-PCRNet). The i-PCRNet uses a modified form of PCRNet as the single pass alignment module in Fig. 2(b). We retain the structure of PCRNet but modify the number of layers. The fully connected layers have three hidden layers with size 1024, 512, 256. Also, there is an additional dropout layer before the output layer, to avoid overfitting. We empirically observe that introducing iterations allows us to use lesser number of hidden layers compared to PCRNet, and yet obtain robust performance.

PointNetLK The PointNetLK was introduced by Aoki et al.. We observe that PointNetLK is just another special case of our framework. If we were to use an inverse compositional Lucas-Kanade algorithm (Baker and Matthews 2004) for aligning the features, while still performing the iterations similar to i-PCRNet, the resulting implementation is PointNetLK.

Pose Parameterization The transformation \mathbf{T} , can be parameterized in a number of different ways. We tried several parameterizations namely Cartesian coordinates and unit quaternions, Euler angles, twist coordinates, 6D continuous parameters (Zhou et al. 2019), and 12D parameters (Pais et al. 2019). Contrary to the observations of Zhou et al., we do not observe any significant improvement in using one over the other.

Loss Function There are several choices for loss functions that can be used to train the networks. We considered three options, Frobenius norm (Aoki et al. 2019), EMD (Yuan et al. 2018a) and chamfer distance (Fan, Su, and Guibas 2017). From Fig. 9(a), we observe that while all three loss functions perform well, CD slightly outperforms the other two.

Training In this work, we use *ModelNet40* dataset (Wu et al. 2015) to train the network. This dataset contains CAD models of 40 different object categories. We uniformly sample points based on face area and then used farthest point algorithm (Eldar et al. 1997) to get a complete point cloud. We train the networks with three different types of datasets as following – (1) Multiple categories of objects and multiple models from each category, (2) Multiple models of a specific category, (3) A single model from a specific category. We choose these 3 cases to showcase the performance of the PointNet-based approaches on data with differing levels of object-specificity.

We train the i-PCRNet with 8 iterations during training, observing that more than 8 produced little improvement to results. In some experiments the training data was corrupted with Gaussian noise, which is discussed in detail in Sec. 4.3. The networks are trained for 300 epochs, using a learning rate of 10^{-1} with an exponential decay rate of 0.7 after every 3×10^6 steps and batch size 32. The network parameters are updated with Adam Optimizer on a single NVIDIA GeForce GTX 1070 GPU and a Intel Core i7 CPU at 4.0GHz.

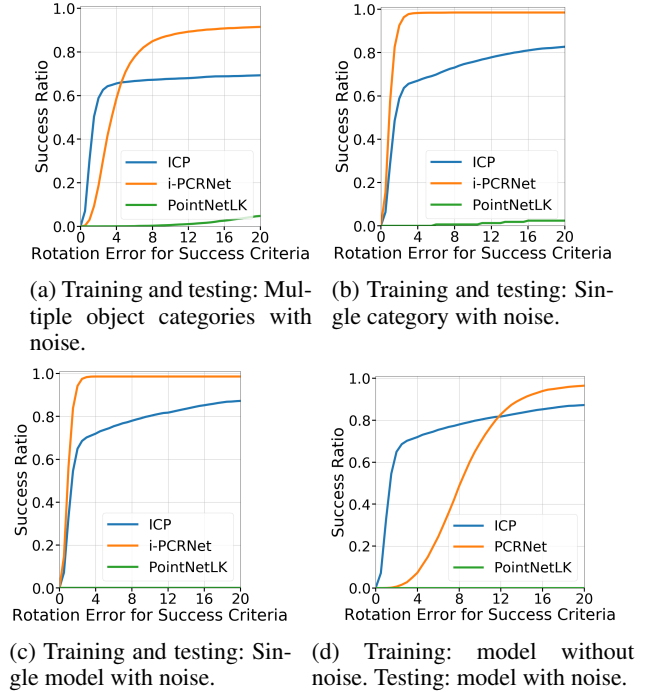


Figure 3: Results for Section 4.3. The y -axis is the ratio of experiments that are successful and the x -axis shows value of the maximum rotation error that qualifies the estimation to be a success. (a), (b) and (c) shows results for comparisons of i-PCRNet with ICP and PointNetLK using three different types of datasets. We observe superior performance of i-PCRNet as our network has more model/category specific information. (d) PCRNet which has not seen noise during training but tested with noisy data also shows good performance and is faster than ICP and PointNetLK.

4 Results

In this section, we compare performance of our networks on test data with multiple object categories, a specific object category, a specific object from training dataset and objects unseen in training. We use models from *ModelNet40* dataset (Wu et al. 2015) for the following experiments. Template point clouds are normalized into a unit box and then their mean is shifted to origin. We randomly choose 5070 transformations with Euler angles in the range of $[-45^\circ, 45^\circ]$ and translation values in the range of $[-1, 1]$ units. We apply these rigid transformations on the template point clouds to generate the source point clouds. We allow a maximum of 20 iterations for both i-PCRNet and PointNetLK while performing tests, while the maximum iterations for ICP was chosen as 100. In addition to maximum iterations, we also use the convergence criteria $\|\mathbf{T}_i \mathbf{T}_{i-1}^{-1} - \mathbf{I}\|_F < \epsilon$, where $\mathbf{T}_i, \mathbf{T}_{i-1} \in SE(3)$ are the transformations predicted in current and previous iterations, and the value of ϵ is chosen to be 10^{-7} .

In order to evaluate the performance of the registration algorithms, we generate plots (see Fig. 3) showing success

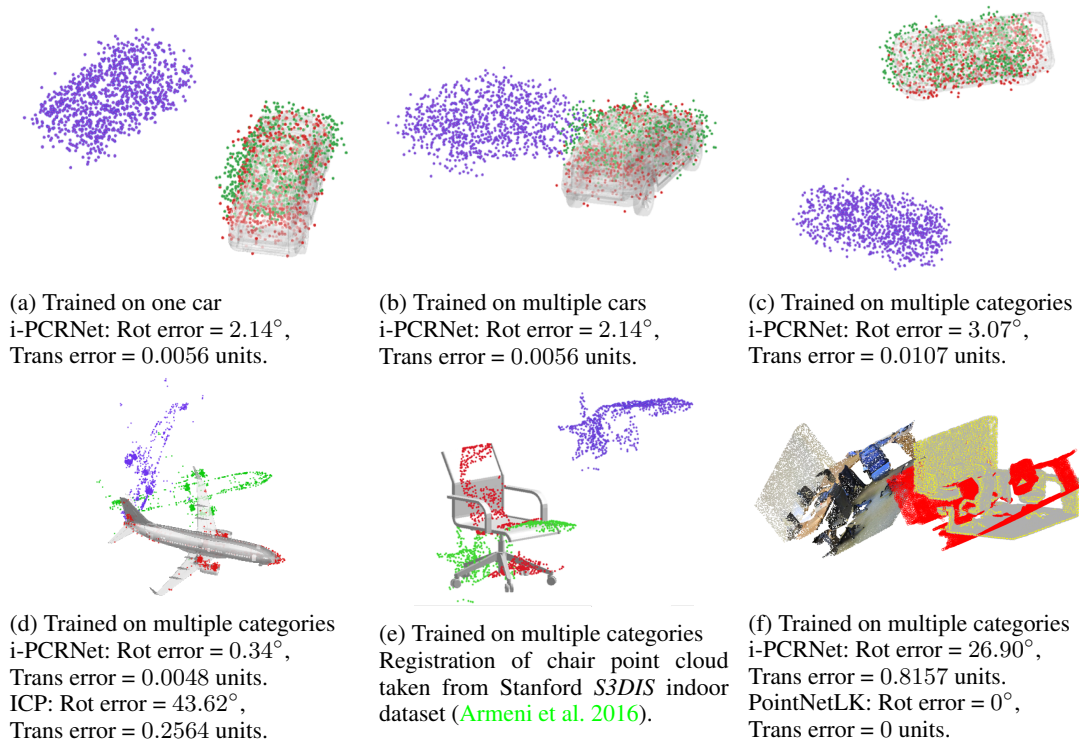


Figure 4: Qualitative results for Section 4. For each example, template is shown by a grey rendered CAD model, purple points show initial position of source and red points show converged results of i-PCRNet trained on data with noise and green points show results of ICP. (d) shows a result with sparse point cloud, (e) shows a result with partial point cloud, and (f) shows a result of unseen category for PointNetLK with yellow points and i-PCRNet with red points. For (a) - (e), where the test data has some representation in training, i-PCRNet performs better. On the other hand, in the case of (f) where the test data is obtained from an RGBD scan and is unseen during training, PointNetLK performs better.

ratio versus success criteria on rotation error (in degrees)¹. We define the area under the curve in these plots, divided by 180 to normalize between 0 and 1, as AUC. AUC expresses a measure of success of registration and so the higher the value of AUC, the better the performance of the network. We measure the misalignment between predicted transformation and ground truth transformation and express it in axis-angle representation and we report the angle as rotation error. As for the translation error, we report the L2 norm of the difference between ground truth and estimated translation vectors.

4.1 Generalizability versus specificity

In the first experiment, i-PCRNet and PointNetLK are trained on 20 different object categories from *ModelNet40* with a total of 5070 models. We perform tests using 100 models chosen from 5 object categories which are not in training data (referred to as unseen categories) with no noise in point clouds. We ensure that same pair of source and template point clouds are used to test all algorithms, for a fair comparison.

We trained i-PCRNet and PointNetLK using multiple object categories and tested them using object categories which are not in training data. There was no noise in source data

¹We define success ratio as the number of test cases having rotation error less than success criteria.

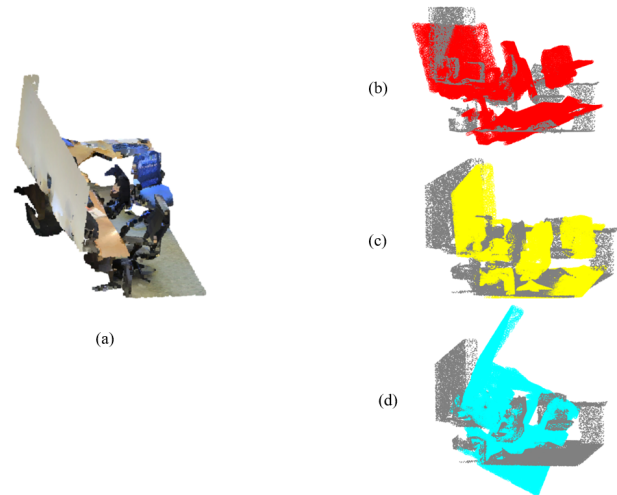


Figure 5: (a) Partial point cloud of office scene from Stanford *S3DIS* indoor dataset (b) red points show registration result of i-PCRNet (19 degrees rotation error) (c) yellow points show registration result of PointNetLK (7 degrees rotation error) (d) cyan points show registration result of 3DSmoothNet (14 degrees rotation error)

during training and testing for this experiment. With these tests, we found that AUC for ICP is 0.802, for i-PCRNet is 0.682 and for PointNetLK it is 0.998.

Upon repeating the experiments by training the networks with objects from the same category as the data being tested on, we observe a massive improvement in the AUC for i-PCRNet, going from 0.682 to 0.972. The AUC for ICP and PointNetLK were similar to earlier at 0.862 and 0.998 respectively, and the AUC of PCRNet was 0.998.

These results emphasize that the i-PCRNet and PCRNet, when retrained with object specific information, provide improved registration results compared to ICP as well as the version trained with multiple categories. Their performance is comparable to PointNetLK when trained with object specific information. However, PointNetLK shows better generalization than i-PCRNet across various object categories and has better performance compared to ICP (as also observed by (Aoki et al. 2019)). We attribute this to the inherent limitation of the learning capacity of PCRNet to large shape variations, while PointNetLK only has to learn the PointNet representation rather than the task of alignment. However, in the next set of experiments, we demonstrate the definite advantages of PCRNet over PointNetLK and other baselines, especially in the presence of noisy data.

4.2 Incomplete point cloud

Extending our discussion on robustness when trained with object specific information, we present results for the networks trained on partial source point cloud data. Fig. 6 shows results for varying percentage of incomplete data in the source point cloud. Note that the network trained with partial data is very robust compared to the one that is trained without any partial data. While ICP performs well in all cases, it is computationally slower than iPCRNet (as discussed later in Sec. 4.4). Further, refining the output of the network with ICP is not always helpful. For instance when the network predicts a wrong pose, ICP refinement can further worsen the alignment as shown in Fig. 6. In case of partial source data, i-PCRNet does not perform very well if it hasn't been trained on the partial data as shown in Fig. 10. This might hint at the object-specificity of this approach.

4.3 Gaussian noise

In order to evaluate robustness of our networks to noise, we perform experiments with Gaussian noise in the source points. For our first experiment, we use dataset as described in Sec. 4.1. We sample noise from a zero mean Gaussian distribution with a standard deviation varying in the range of 0 to 0.04 units. During testing, we compare the methods with noise in source data for each algorithm. We ensured that the dataset has the same pairs of source and template point clouds for a fair comparison.

For the second experiment, we train the networks only on a specific object category with added Gaussian noise. We test them on the 150 models of the same category with Gaussian noise. In a similar manner, for the third experiment, we train and test the networks on only one noisy model. In all these cases, i-PCRNet is most robust to Gaussian noise, with higher number of successful test cases having

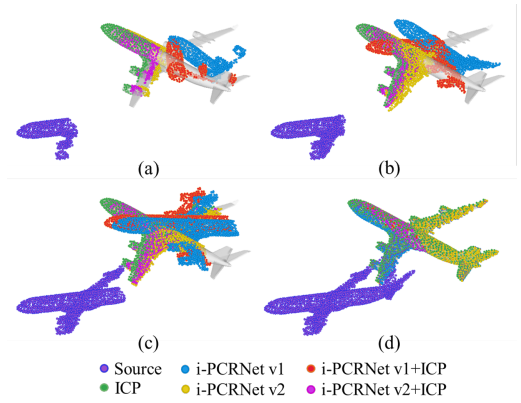


Figure 6: Results for Sec. 4.2. Rotation and translation error for registering incomplete source point cloud to a template model of airplane. The i-PCRNet v1 and i-PCRNet v2 are trained without and with incomplete source data, respectively. (a) 70% incompleteness, (b) 50% incompleteness, (c) 20% incompleteness, and (d) complete source data. The performance of i-PCRNet v2 is comparable to ICP (and much better than i-PCRNet v1) even with large amounts of missing points, while being computationally faster than ICP. The ICP refinement produces an improvement only for i-PCRNet v2 and not i-PCRNet v1, since the alignment of i-PCRNet v1 is poor and beyond ICP's capability of refinement.

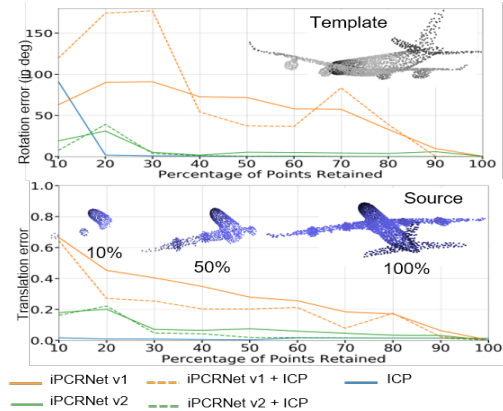


Figure 7: Rotation and translation error for registering incomplete source point cloud to a template model of airplane. The i-PCRNet v1 and i-PCRNet v2 are trained without and with incomplete source data, respectively. The performance of i-PCRNet v2 is comparable to ICP (and much better than i-PCRNet v1) even with large amounts of missing points, while being computationally faster than ICP. The ICP refinement produces an improvement only for i-PCRNet v2 and not i-PCRNet v1, since the alignment of i-PCRNet v1 is poor and beyond ICP's capability of refinement.

smaller rotation error as compared to ICP and PointNetLK (see Fig. 3a 3b 3c). It is worth noting that PointNetLK is very sensitive to noisy data.

Finally, we compare PCRNet that is trained without noise and tested on noisy data, with ICP and PointNetLK. While

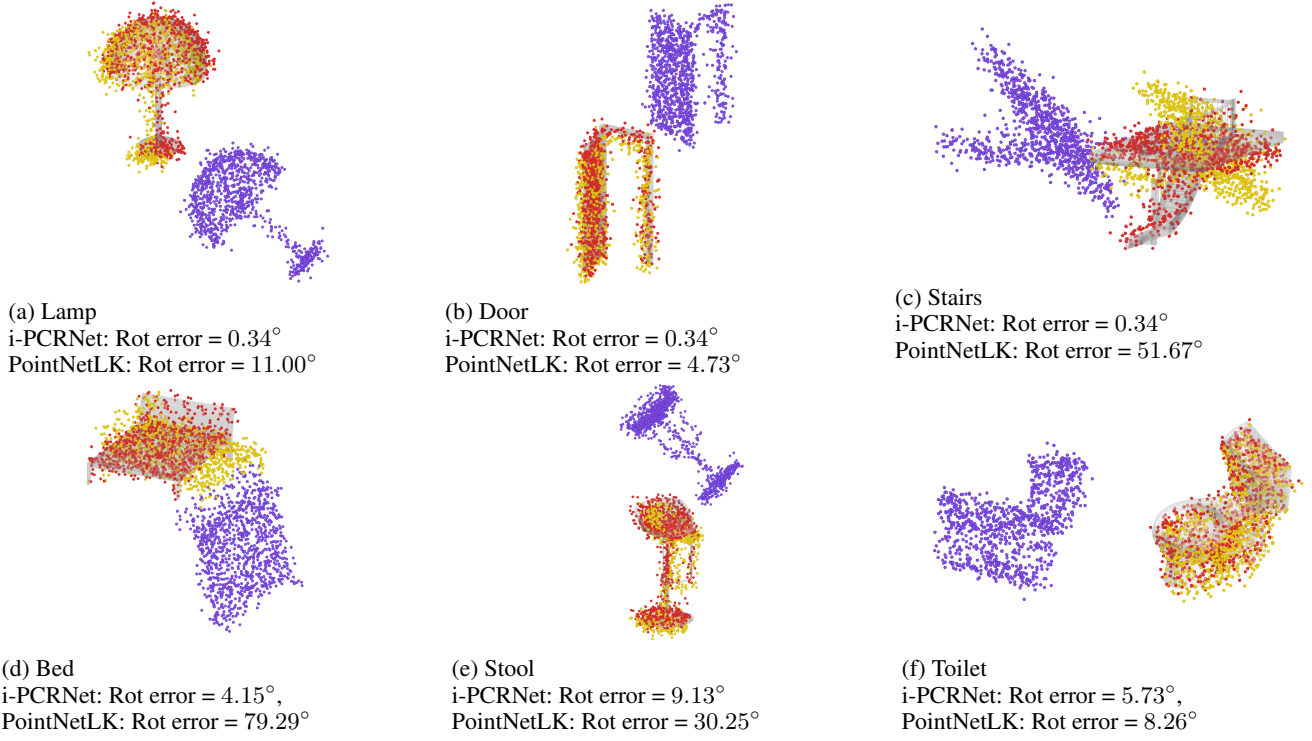


Figure 8: Results for noisy source point clouds. For each example, the template is visualized by a grey rendered CAD model, purple points show initial position of source, green points show results of ICP, red points show converged results of i-PCRNet trained on data with noise, yellow points show the results of PointNetLK trained on noisy data.

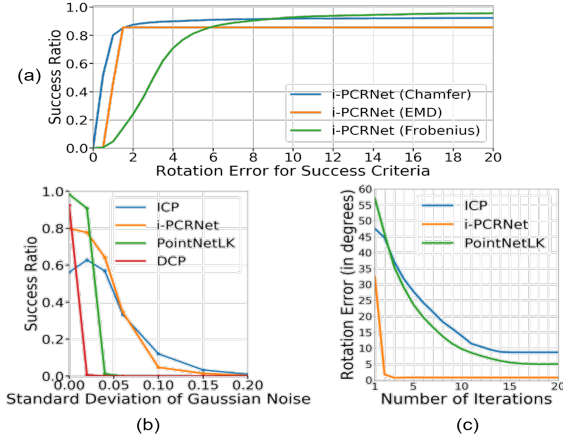


Figure 9: (a) Performance of i-PCRNet for different choices of loss functions. Chamfer loss shows best performance in our experiments. (b) Performance of ICP, i-PCRNet, PointNetLK and DCP for different levels of noise in source point cloud. DCP and PointNetLK are very sensitive to noise and perform the worst. i-PCRNet is very robust to noise in the levels that it has observed during training. (c) Rotation error versus the number of iterations performed to find the pose. i-PCRNet aligns source and template point clouds in least amount of iterations.

not being as good as ICP, PCRNet is still competitive, and performs much better than PointNetLK (See Fig. 3d). We present qualitative results in Fig. 4 using i-PCRNet trained on multiple datasets and testing with noisy data. As expected, the accuracy of i-PCRNet is highest when trained on the same model that it is being tested on. The accuracy drops only a little when trained on multiple models and multiple categories, showing a good generalization as long as there is some representation of the test data in the training. Fig. 8 shows an extension of our discussion where we observe that i-PCRNet performs better than PointNetLK when dealing with noisy data.

Fig. 9(b) shows success ratio versus the amount of noise added to source point clouds during testing. DCP, i-PCRNet and PointNetLK are trained on multiple object categories with Gaussian noise having a maximum standard deviation of 0.04. We observe a sudden drop in the performance of PointNetLK and DCP as the standard deviation for noise increases above 0.02. On the other hand, i-PCRNet performs best in the neighbourhood of the noise range that it was trained on (0.02-0.06), and produces results comparable to ICP beyond that noise level. This shows that i-PCRNet is more robust to noise as compared to PointNetLK. Fig. 9(c) shows the rotation error versus number of iterations in for the different methods. Notice that the i-PCRNet takes only 3 iterations to get close to convergence, compared to the other methods that take upwards of 15 iterations.

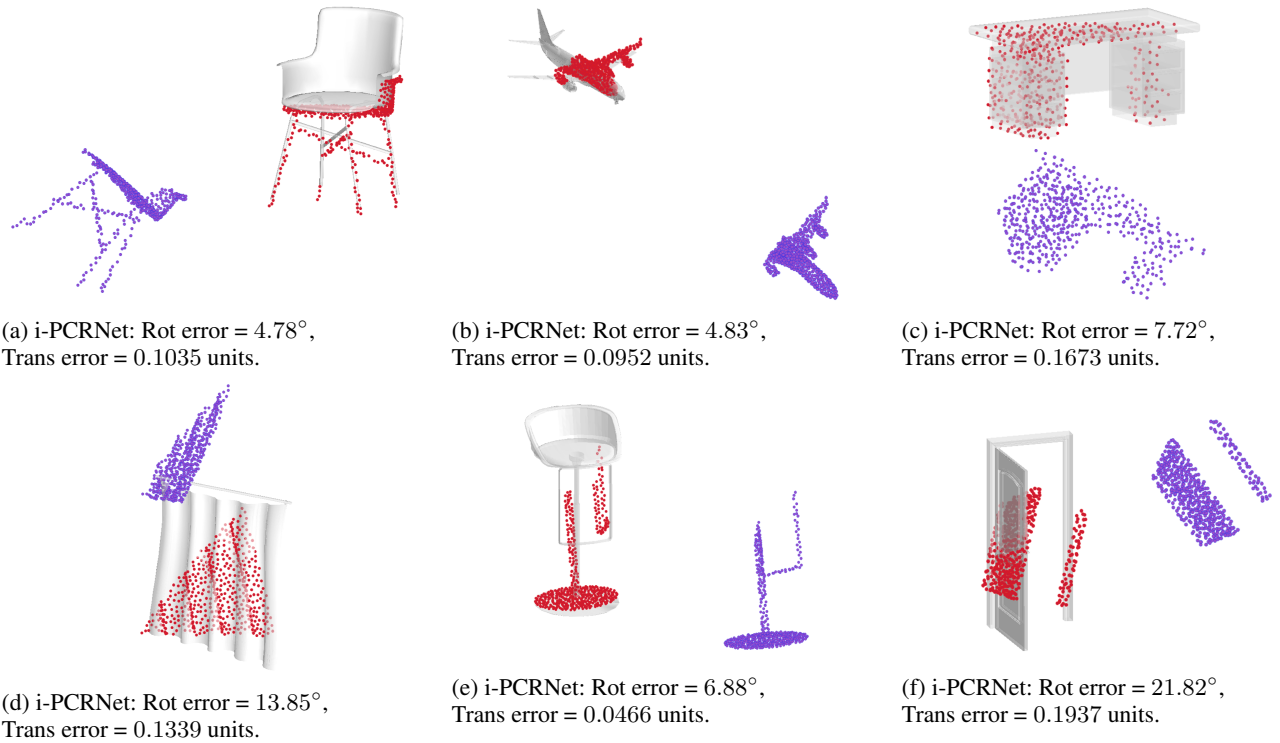


Figure 10: Qualitative results for partial point clouds. For each example, template is shown by a grey rendered CAD model, purple points show initial position of source and red points show converged results of i-PCRNet trained on partial data.

4.4 Computation speed comparisons

We use a testing dataset with only one model of car from *ModelNet40* dataset, with Gaussian noise in the source data. We apply 100 randomly chosen transformations with Euler angles in range of $[-45^\circ, 45^\circ]$ and translation values in range of $[-1, 1]$ units. All the networks are trained using multiple models of same category (i.e. car). We compared the performance of i-PCRNet, PCRNet, PointNetLK, DCP, ICP and Go-ICP, as shown in Table 1. We also develop a variant of i-PCRNet (we refer to this as VoxReg), where the PointNet module is replaced with a VoxNet (Maturana and Scherer 2015). The comparison methods were chosen to cover a wide spectrum of registration methods, including conventional approaches and learning-based approaches. The learning-based methods use different embeddings such as pointNet, dynamic graph and voxels.

The results demonstrate that Go-ICP converges to a globally optimal solution in all cases with a very small rotation error and translation error, but the time taken is three orders of magnitude more than i-PCRNet and five orders of magnitude more than PCRNet. The VoxReg has an accuracy and computation time similar to ICP. The i-PCRNet has an accuracy similar to Go-ICP, but is computationally much faster, allowing for use in many practical applications. Further, while PCRNet is not as accurate as i-PCRNet, the accuracy may be good enough for a pre-aligning step in applications such as object detection and segmentation (Yuan et al. 2018a).

Table 1: Results from Section 4.4.

	Rot. Error (deg)		Trans. Error ($\times 10^{-2}$)		Time (ms)		AUC
	μ	σ	μ	σ	μ	σ	
PCRNet	8.82	4.82	0.77	0.08	1.89	0.39	0.95
i-PCRNet	1.03	2.56	0.85	0.24	146	30.40	0.99
PtNetLK	51.80	29.63	87.83	0.54	234	41.60	0.70
ICP	11.87	31.87	2.82	3.92	407	128.0	0.93
DCP	24.15	14.65	0.74	0.42	27.4	1.55	0.86
VoxReg	13.97	10.67	5.61	3.27	459	88.4	0.92
Go-ICP	0.45	0.19	0.16	0.07	2.7×10^5	1.5×10^5	1.00

4.5 Sparse Data

We observe from Fig. 11 that i-PCRNet trained on sparse data performs better on testing with sparse data.

5 Model replacement using segmentation

To show qualitative performance on real-world data, we demonstrate the use of i-PCRNet to find the pose and modify the models in an indoor point cloud dataset (Armeni et al. 2016). We use the semantic segmentation network introduced in PointNet (Qi et al. 2017a) to segment a chair from a scene chosen from the Stanford *S3DIS* indoor dataset. We then register it to a chair model from *ModelNet40* dataset using i-PCRNet, which was trained on multiple object categories with noise.

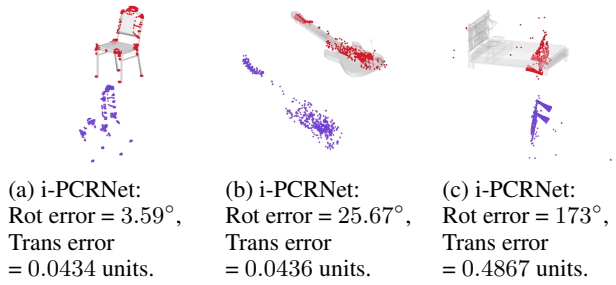


Figure 11: Qualitative results for sparse point clouds. For each example, template is shown by a grey rendered CAD model, purple points show initial position of source and red points show converged results of i-PCNet trained on sparse point clouds

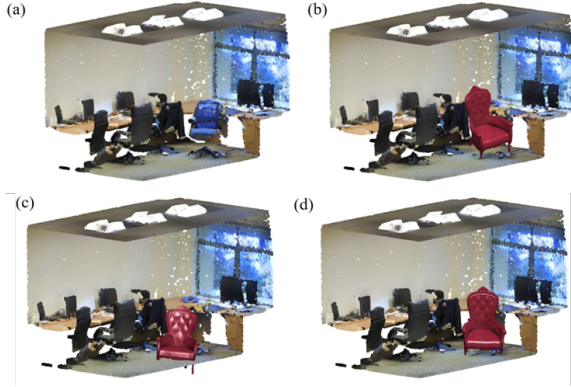


Figure 12: Replacement of chairs in office scene from Stanford S3DIS indoor dataset. Red leather chairs shows the replaced chair from ModelNet40 (a) Original scene. Red leather chair replaced by using registration from (b) ICP, (c) Global registration method, and (d) i-PCNet.

We replace the original chair with a different chair using the pose obtained from i-PCNet as shown in Fig. 12. Notice that both ICP and global registration method (Izatt, Dai, and Tedrake 2017) fail to register the chair to the right pose, while i-PCNet accurately registers the point clouds.

6 Discussions and future work

This work presents a novel data-driven framework for performing registration of point clouds using the PointNet representation.

The framework illustrates how data-driven techniques may be used to learn a distribution over appearance variation in point cloud data, including noisy data or category-specificity, and perform better at test time using such a learned prior. The framework can be implemented in an iterative manner to obtain highly accurate estimates comparable to global registration methods. The framework could also be implemented without the iterations, but with deeper layers to produce two to five orders of magnitude speed improvement compared to popular registration methods. Finally, this framework also puts into context other recent PointNet-based registration methods in literature such as the

PointNetLK.

Future work would involve integration into larger deep neural network systems, for tasks such as multi-object tracking, style transfer, mapping, etc. Future work may explore the limitations of the learning capacity of the fully-connected registration layers to the size of data distribution.

References

- [Angelina Uy and Hee Lee 2018] Angelina Uy, M., and Hee Lee, G. 2018. Pointnetvlad: Deep point cloud based retrieval for large-scale place recognition. In *Proc. of CVPR*, 4470–4479. 2
- [Aoki et al. 2019] Aoki, Y.; Goforth, H.; Srivatsan, R. A.; and Lucey, S. 2019. Pointnetlk: Robust & efficient point cloud registration using pointnet. In *Proc. CVPR*, 7163–7172. 1, 2, 4, 6
- [Armeni et al. 2016] Armeni, I.; Sener, O.; Zamir, A. R.; Jiang, H.; Brilakis, I.; Fischer, M.; and Savarese, S. 2016. 3d semantic parsing of large-scale indoor spaces. In *Proceedings of CVPR*. 5, 8
- [Baker and Matthews 2004] Baker, S., and Matthews, I. 2004. Lucas-Kanade 20 years on: A unifying framework. *IJCV* 56(3):221–255. 2, 3, 4
- [Besl and McKay 1992] Besl, P. J., and McKay, N. D. 1992. Method for registration of 3-d shapes. In *Sensor Fusion IV: Control Paradigms and Data Structures*, volume 1611, 586–607. International Society for Optics and Photonics. 1, 2, 3
- [Bristow, Valmadre, and Lucey 2015] Bristow, H.; Valmadre, J.; and Lucey, S. 2015. Dense semantic correspondence where every pixel is a classifier. In *Proceedings of ICCV*, 4024–4031. 2
- [Elbaz, Avraham, and Fischer 2017] Elbaz, G.; Avraham, T.; and Fischer, A. 2017. 3d point cloud registration for localization using a deep neural network auto-encoder. In *Proc. of CVPR*, 4631–4640. 2
- [Eldar et al. 1997] Eldar, Y.; Lindenbaum, M.; Porat, M.; and Zeevi, Y. Y. 1997. The farthest point strategy for progressive image sampling. *IEEE Transactions on Image Processing* 6(9):1305–1315. 4
- [Fan, Su, and Guibas 2017] Fan, H.; Su, H.; and Guibas, L. J. 2017. A point set generation network for 3d object reconstruction from a single image. In *Proc. of CVPR*, 605–613. 4
- [Gelfand et al. 2005] Gelfand, N.; Mitra, N. J.; Guibas, L. J.; and Pottmann, H. 2005. Robust global registration. In *Symposium on geometry processing*, volume 2, 5. Vienna, Austria. 1, 2
- [Georgakis et al. 2018] Georgakis, G.; Karanam, S.; Wu, Z.; and Kosecka, J. 2018. Matching RGB Images to CAD Models for Object Pose Estimation. *arXiv preprint arXiv:1811.07249*. 2
- [Gojcic et al. 2019] Gojcic, Z.; Zhou, C.; Wegner, J. D.; and Wieser, A. 2019. The perfect match: 3d point cloud matching with smoothed densities. In *Proc. CVPR*, 5545–5554. 1
- [Guo et al. 2014] Guo, Y.; Bennamoun, M.; Soheli, F.; Lu, M.; and Wan, J. 2014. 3D object recognition in cluttered scenes with local surface features: a survey. *IEEE Transactions on Pattern Analysis and Machine Intelligence* 36(11):2270–2287. 2
- [Held, Thrun, and Savarese 2016] Held, D.; Thrun, S.; and Savarese, S. 2016. Learning to track at 100 fps with deep regression networks. In *ECCV*, 749–765. Springer. 3
- [Insafutdinov and Dosovitskiy 2018] Insafutdinov, E., and Dosovitskiy, A. 2018. Unsupervised learning of shape and pose with differentiable point clouds. In *Advances in Neural Information Processing Systems*, 2802–2812. 3
- [Izatt, Dai, and Tedrake 2017] Izatt, G.; Dai, H.; and Tedrake, R. 2017. Globally optimal object pose estimation in point clouds

- with mixed-integer programming. In *International Symposium on Robotics Research*. 2, 9
- [Li et al. 2018] Li, Y.; Wang, G.; Ji, X.; Xiang, Y.; and Fox, D. 2018. DeepIM: Deep iterative matching for 6d pose estimation. In *Proceedings of ECCV*, 683–698. 3
- [Liu, Qi, and Guibas 2019] Liu, X.; Qi, C. R.; and Guibas, L. J. 2019. Flownet3d: Learning scene flow in 3d point clouds. In *Proc. CVPR*, 529–537. 2
- [Lu et al. 2019] Lu, W.; Wan, G.; Zhou, Y.; Fu, X.; Yuan, P.; and Song, S. 2019. DeepICP: An End-to-End Deep Neural Network for 3D Point Cloud Registration. *arXiv preprint arXiv:1905.04153*. 2
- [Lucas and Kanade 1981] Lucas, B. D., and Kanade, T. 1981. An iterative image registration technique with an application to stereo vision. *Proc. of IJCAI*. 2
- [Makadia, Patterson, and Daniilidis 2006] Makadia, A.; Patterson, A.; and Daniilidis, K. 2006. Fully automatic registration of 3D point clouds. In *Computer Vision and Pattern Recognition, 2006 IEEE Computer Society Conference on*, volume 1, 1297–1304. IEEE. 2
- [Maron et al. 2016] Maron, H.; Dym, N.; Kezurer, I.; Kovalsky, S.; and Lipman, Y. 2016. Point registration via efficient convex relaxation. *ACM TOG* 35(4):73. 2
- [Maturana and Scherer 2015] Maturana, D., and Scherer, S. 2015. Voxnet: A 3d convolutional neural network for real-time object recognition. In *IROS*, 922–928. 1, 2, 8
- [Ovsjanikov et al. 2010] Ovsjanikov, M.; M  rigot, Q.; M  moli, F.; and Guibas, L. 2010. One point isometric matching with the heat kernel. *Computer Graphics Forum* 29(5):1555–1564. 2
- [Pais et al. 2019] Pais, G. D.; Miraldo, P.; Ramalingam, S.; Govindu, V. M.; Nascimento, J. C.; and Chellappa, R. 2019. 3DRegNet: A Deep Neural Network for 3D Point Registration. *arXiv preprint arXiv:1904.01701*. 3, 4
- [Qi et al. 2017a] Qi, C. R.; Su, H.; Mo, K.; and Guibas, L. J. 2017a. Pointnet: Deep learning on point sets for 3d classification and segmentation. *Proc. CVPR* 1(2):4. 1, 2, 3, 8
- [Qi et al. 2017b] Qi, C. R.; Yi, L.; Su, H.; and Guibas, L. J. 2017b. Pointnet++: Deep hierarchical feature learning on point sets in a metric space. In *Advances in Neural Information Processing Systems*, 5099–5108. 1, 2
- [Qi et al. 2018] Qi, C. R.; Liu, W.; Wu, C.; Su, H.; and Guibas, L. J. 2018. Frustum pointnets for 3d object detection from RGB-D data. In *Proc. of CVPR*, 918–927. 1, 2
- [Rusinkiewicz and Levoy 2001] Rusinkiewicz, S., and Levoy, M. 2001. Efficient variants of the ICP algorithm. In *3dim*, volume 1, 145–152. 2
- [Rusu, Blodow, and Beetz 2009] Rusu, R. B.; Blodow, N.; and Beetz, M. 2009. Fast point feature histograms (FPFH) for 3D registration. In *ICRA*, 3212–3217. 1, 2
- [Srivatsan et al. 2019] Srivatsan, R. A.; Zevallos, N.; Vagdari, P.; and Choset, H. 2019. Registration with a small number of sparse measurements. *IJRR*. 2
- [Vongkulbhisal et al. 2018] Vongkulbhisal, J.; Irastorza Ugalde, B.; De la Torre, F.; and Costeira, J. P. 2018. Inverse composition discriminative optimization for point cloud registration. In *Proc. of CVPR*, 2993–3001. 2
- [Wang and Solomon 2019] Wang, Y., and Solomon, J. M. 2019. Deep Closest Point: Learning Representations for Point Cloud Registration. *arXiv preprint arXiv:1905.03304*. 1, 3
- [Wang et al. 2018] Wang, Y.; Sun, Y.; Liu, Z.; Sarma, S. E.; Bronstein, M. M.; and Solomon, J. M. 2018. Dynamic graph CNN for learning on point clouds. *arXiv preprint arXiv:1801.07829*. 1, 2
- [Wang et al. 2019] Wang, C.; Xu, D.; Zhu, Y.; Mart  n-Mart  n, R.; Lu, C.; Fei-Fei, L.; and Savarese, S. 2019. Densefusion: 6D object pose estimation by iterative dense fusion. In *Proc. CVPR*, 3343–3352. 3
- [Wu et al. 2015] Wu, Z.; Song, S.; Khosla, A.; Yu, F.; Zhang, L.; Tang, X.; and Xiao, J. 2015. 3d shapenets: A deep representation for volumetric shapes. In *Proc. CVPR*, 1912–1920. 1, 2, 4
- [Xiang et al. 2018] Xiang, Y.; Schmidt, T.; Narayanan, V.; and Fox, D. 2018. PoseCNN: A Convolutional Neural Network for 6D Object Pose Estimation in Cluttered Scenes. In *RSS*. 2
- [Yang et al. 2016] Yang, J.; Li, H.; Campbell, D.; and Jia, Y. 2016. Go-ICP: A globally optimal solution to 3D ICP point-set registration. *IEEE trans. on pattern analysis and machine intelligence* 38(11):2241–2254. 1, 2
- [Yew and Lee 2018] Yew, Z. J., and Lee, G. H. 2018. 3dfeat-net: Weakly supervised local 3d features for point cloud registration. In *ECCV*, 630–646. 2
- [Yuan et al. 2018a] Yuan, W.; Held, D.; Mertz, C.; and Hebert, M. 2018a. Iterative transformer network for 3d point cloud. *arXiv preprint arXiv:1811.11209*. 1, 2, 4, 8
- [Yuan et al. 2018b] Yuan, W.; Khot, T.; Held, D.; Mertz, C.; and Hebert, M. 2018b. PCN: Point Completion Network. In *3DV*. 2
- [Zhou and Tuzel 2018] Zhou, Y., and Tuzel, O. 2018. Voxnet: End-to-end learning for point cloud based 3d object detection. In *Proc. CVPR*, 4490–4499. 2
- [Zhou et al. 2019] Zhou, Y.; Barnes, C.; Lu, J.; Yang, J.; and Li, H. 2019. On the continuity of rotation representations in neural networks. In *Proc. CVPR*, 5745–5753. 2, 4